附件一

行政院國家科學委員會補助專題研究計畫 ■ 成 果 報 告 □期中進度報告

旋翼型無人載具之非線性動態模擬

Nonlinear Dynamics of Unmanned Aerial Helicopter

計畫類別：■ 個別型計畫　　□ 整合型計畫
計畫編號：NSC 96 － 2623 － 7 － 032 － 001 － D
執行期間：　　96 年 1 月 1 日至 96 年 12 月 31 日

計畫主持人：蕭富元　博士
共同主持人：
計畫參與人員：曾奕智、陳彥熹、陳延詮、朱崇傑

成果報告類型(依經費核定清單規定繳交)：□精簡報告　■完整報告

本成果報告包括以下應繳交之附件：
□赴國外出差或研習心得報告一份
□赴大陸地區出差或研習心得報告一份
□出席國際學術會議心得報告及發表之論文各一份
□國際合作研究計畫國外研究報告書一份

處理方式：除產學合作研究計畫、提升產業技術及人才培育研究計畫、列管計畫及下列情形者外，得立即公開查詢
□涉及專利或其他智慧財產權，□一年□二年後可公開查詢

執行單位：淡江大學航太系

旋翼型無人載具之非線性動態模擬

NONLINEAR DYNAMICS OF UNMANNED AERIAL HELICOPTER

淡江大學航空太空工程學系
研究生：曾奕智、陳彥熹
計劃主持人：蕭富元 博士

中華民國九十七年三月

摘要

本計劃在探討發展小型無人直昇機“翔蛉”(H-Ling，爲雷虎翼手龍90級) 的參數化模型及利用各種系統鑑別的技術來鑑別參數，包括ARX、CIFER 和 PEM。 此項計畫的最終目標是建立一架自主飛行旋翼機。 我們首先簡短回顧了小型直昇機的運動數學式，然後簡單介紹 PEM 的數學原理。藉由收集到的試飛數據，我們將直昇機的參數全數鑑別出來。 本文亦提供利用各種鑑別理論所得的圖表，來顯示這些結果的一致性， 也利用控制器的成戊]計，間接證明這些結果的正確性。 最後列出已找出的非線性模型，未來將用PEM來對非線性模型做系統鑑別。

關鍵字: 無人直昇機(UAH)、系統鑑別、雷虎翼手龍90無人直昇機、預測誤差估測法(PEM) ,非線性系統

Abstract

In this project we are going to develop a parameterized model for a small-scale unmanned helicopter H-Ling (a Thunder Tiger Raptor-90) and its identification using various techniques, including ARX, CIFER and PEM. The ultimate goal of this project is to extend the current work to build a fully functional autonomous rotorcraft. The equations of motion of a small-scaled rotorcraft are briefly reviewed first. We then briefly introduce the mathematics of PEM. With the flight test data, we obtain the identified parameters of the dynamical model. Numerical simulations and table of identified parameters are provided to show the consistency and correctness of our results. List the nonlinear model that has already been found out finally,and will identification the nonlinear model with PEM in the future.

Keyword: Unmanned Aerial Helicopter (UAH), System Identification, Raptor-90, Prediction Error Estimation Methods (PEM),nonlinear system

Nomenclature

Symbol

β	blade flapping angle
β_0	rotor blade coning angle
β_{1c}	rotor blade longitudinal $^\circ$ apping angle
β_{1s}	rotor blade lateral $^\circ$ apping angle
δ_{col}	collective control input
δ_{lat}	lateral control input
δ_{lon}	longitudinal control input
δ_{ped}	pedal control input
a_0	Coning angle
a_1	Slope of lift curve
a	First harmonic coefficient of longitudinal blade flapping with respect to shaft
A_1	First lateral harmonic of blade feathering
A_b	Area of blades
b	First harmonic coefficient of lateral blade flapping with respect to shaft
B_1	First longitudinal coefficient of blade feathering
C_p	Coefficient of power
C_Q	Coefficient of torque
C_T	Coefficient of thrust
p	Roll rate
q	Pitch rate
r	Yaw rate
R	Rotor radius
u, v, ω	translational velocity of helicopter about fuselage
θ_1	Blade twist

λ'	Inflow ratio with respect to tip path plane
μ	Tip speed ratio
σ	Solidity of rotor
ρ	Density of air
Ω	Rotational speed of rotor
τ_f, τ_s	main blade and flybar time constant
r_b	blade radial distance
I_{xx}, I_{yy}, I_{zz}	Principle moment of inertia
L, M, N	External resultant moment
X, Y, Z	External resultant force
$u(t)$	input variable
$y(t)$	output variable
X_u, X_a, etc	force derivatives of X direction force
Y_v, Y_b, etc	force derivatives of Y direction force
Z_u, Z_w, etc	force derivatives of Z direction force
L_u, L_v, L_b, etc	moment derivatives of rolling moment
M_u, M_v, M_a, etc	moment derivatives of pitchling moment
N_r, N_{ped}	moment derivatives of yawing moment

Subscripts

H	Horizontal stabilizer
M	Main rotor
Q	torque
T	Tail rotor

Chapter 1

Introduction

1.1 Motivation

In this project we are going to develop a parameterized model for a small-scale unmanned helicopter H-Ling (a Thunder Tiger Raptor-90) and its identification using various techniques. The ultimate goal of this project is to extend the current work to build a fully functional autonomous rotorcraft. The development of unmanned helicopters is of great interest among researchers resulted from their no need of human crewmembers and take-off runways, leading to broad applications of this vehicle, such as executing dangerous missions in many aspects.

1.2 Literature Review

The development of unmanned helicopters starts in early 1990's including the establishment of precise dynamics model and implementation of control law[1]. Due to the complexity of a helicopter the dynamics model is usually obtained through system identification techniques, using experimental

input-output data collected from a plant to produce a mathematical representation of the system's dynamics. In the 1980s, the US Army/NASA developed a tool named CIFER (Comprehensive Identification from FrEquency Responses) for the rotorcraft identification, and CIFER was successfully applied by Mettler to identify a small-scaled helicopter [3, 8]. In 2006 Tseng and Hsiao use ARX, collaborated with CIFER, to identify the dynamics of H-Ling [13]. However, their work requires sophisticated maneuvers in flight test to stimulate spectra responses, and that increases difficulties in flight test. As a result, the application of an alternative identification method, named PEM (Prediction Error Estimation Methods), is discussed in this project.

1.3 Research Methodology

Having applied ARX and CIFER to identify the dynamics of H-Ling, we intend to discuss the application of the Prediction Error Estimation Methods (PEM) in this project. The equations of motion of a small-scaled rotorcraft are briefly reviewed first. We then briefly introduce the mathematics of ARX and PEM. With the flight test data, we obtain the identified parameters of the dynamical model. Those parameters are compared with what has been identified through different algorithms previously, and shown consistency. Although a linearized model is applied currently, the introduction of PEM can extend the current work to the nonlinear scheme later.Our method is linearization of a helicopter dynamic model , but If want to receive more parameters ,most be identification the nonlinear dynamic model .Because the ARX and CIFER is not suitable for nonlinear

model.So we will identification nonlinear system model with Prediction Error Estimation Methods (PEM) in the future.The system dynamics defined for PEM can be arbitrary. Therefore, it is eligible for identifying a nonlinear system [15]. We have already found out the nonlinear parameter that need be identification now. It will introduce in this project.

Chapter 2

Dynamics Model

As shown in Fig. 2.2. The x axis points toward the front of the fuselage, the z axis points downward, and the y axis completes the triad.In Fig.2.1 the dynamics of a small-scaled rotorcraft is usually composed of four parts: A. the fuselage, modeled as a rigid body; B. the main blades, offering lift and thrust; C. pedal blades along with gyroscope, controlling the yawing motion; D. flybar (also known as a stabilizer bar), stabilizing the rolling and pitching motion [5]- [7].

Figure 2.1: Thunder Tiger Raptor-90 mini-helicopter

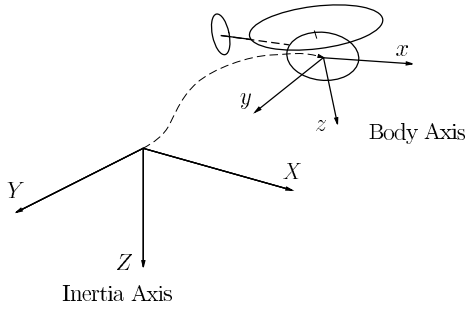

Figure 2.2: The Axis System

2.1 Equations of Motion

The helicopter we select to investigate is the Thunder Tiger Raptor 90, shown in Fig. 2.1. To derive the equations of motion, we define an inertial frame and a body fixed frame, shown in Fig. 2.2. The equations of motion (EOM) with respect to the body-fixed reference frame attached with the fuselage are given by

$$m\dot{v} + m(\omega \times v) = F \tag{2.1}$$

$$I\dot{\omega} + (\omega \times I\omega) = M \tag{2.2}$$

where $\mathbf{F} = \begin{bmatrix} X & Y & Z \end{bmatrix}^T$ is external forces acting on vehicle, $\mathbf{M} = \begin{bmatrix} L & M & N \end{bmatrix}^T$ is external moments acting on vehicle,$\mathbf{v} = \begin{bmatrix} u & v & w \end{bmatrix}^T$ is the vector of body velocities,$\omega = \begin{bmatrix} p & q & r \end{bmatrix}^T$ is the vector of angular rate, and $\mathbf{I} = \text{diag}(I_{xx}, I_{yy}, I_{zz})$ denotes the principle moment of inertia [1, 5, 9–11].
Eq. (2.1) produces the three differential equations describing the helicopter's translational motion about its three reference axes, and can be expanded as

$$\dot{u} = vr - wq - g\sin\theta + X/m \tag{2.3}$$

$$\dot{v} = wp - ur + g\sin\phi\cos\theta + Y/m \tag{2.4}$$

$$\dot{w} = uq - vp + g\cos\phi\cos\phi + Z/m \tag{2.5}$$

Eq. (2.2) produces the three differential equations describing the helicopter's rotational motion about its three reference axes, and can be expanded as

$$\dot{p} = -qr(I_{yy} - I_{zz})/I_{xx} + L/I_{xx} \tag{2.6}$$

$$\dot{q} = -pr(I_{zz} - I_{xx})/I_{yy} + M/I_{yy} \tag{2.7}$$

$$\dot{r} = -pq(I_{xx} - I_{yy})/I_{zz} + N/I_{zz} \tag{2.8}$$

The forces and moments can be further expanded in terms of the coupling effects between main blades and flybar, as well as the pedal blades and the gyroscopic feedback. Having linearized about the state of hover, i.e.,$u = v = \omega = 0$,$p = q = r = 0$, Eq. (2.3) to (2.8) can be re-written as a multiple-input- multiple-output , linear time invariant system, given by:

$$\begin{aligned} \dot{\mathbf{x}} &= \mathbf{A}\mathbf{x} + \mathbf{B}\mathbf{u} \\ \mathbf{y} &= \mathbf{C}\mathbf{x} \end{aligned} \tag{2.9}$$

where $\mathbf{x}$ is the state vector, and $\mathbf{u}$ is the control input vector, including cyclic lateral input δ_{lat} , cyclic longitudinal input δ_{lon}, collective pitch input δ_{col}, and pedal input δ_{ped}.The details of Eq. (2.9) are given in the appendix and Refs. [6, 10, 13].

The Euler angles then can be computed from the rotation rates, given by:

$$\dot{\phi} = p + q\sin\phi\tan\theta + r\cos\phi\tan\theta \tag{2.10}$$

$$\dot{\theta} = q\cos\phi - r\sin\phi \tag{2.11}$$

$$\dot{\psi} = q\sin\phi\sec\theta + r\cos\phi\sec\theta \tag{2.12}$$

2.2 Linearizatiom of the Equations of Motion

$$\delta\dot{u} = (-w_0\delta q + \delta w q_0 + v_0\delta r + \delta v r_0) + \Delta X/m \tag{2.13}$$

$$\delta\dot{v} = (-v_0\delta r + \delta u r_0 + w_0\delta p + \delta w p_0) + \Delta Y/m \tag{2.14}$$

$$\delta\dot{w} = (-v_0\delta p + \delta v p_0 + u_0\delta q + \delta u q_0) + \Delta Z/m \tag{2.15}$$

$$\delta\dot{p} = (-q_0\delta r - \delta q r_0)(I_{yy} - I_{zz})/I_{xx} + \Delta L/I_{xx} \tag{2.16}$$

$$\delta\dot{q} = (-p_0\delta r - \delta p r_0)(I_{zz} - I_{xx})/I_{yy} + \Delta M/I_{yy} \tag{2.17}$$

$$\delta\dot{r} = (-p_0\delta q - \delta p q_0)(I_{xx} - I_{yy})/I_{zz} + \Delta N/I_{zz} \tag{2.18}$$

where the $\Delta X, \Delta Y, \Delta Z$ are external forces and the $\Delta L, \Delta M, \Delta N$ are external moments .and among them

$$\Delta X = \frac{\partial X}{\partial u}\delta u + \frac{\partial X}{\partial v}\delta v + \cdots + \frac{\partial X}{\partial \delta_{lat}}\delta_{lat} + \frac{\partial X}{\partial \delta_{lon}}\delta_{lon} + \cdots \tag{2.19}$$

where the subscrips are the partial derivatives , such as $X_u \equiv \frac{\partial X}{\partial u}$, etc

2.3 Rotor Tip-Path-Plane Equation

The flapping motion is a 2π-periodic function .Assume the blade is a rigid-body with small flapping angle β , and small effective aerodynamics. The blade equation as a function of blade azimuth angle $\Psi = \Omega t$ show Fig.2.5 is given by :

$$\beta'' + \lambda_\beta^2 \beta = \frac{1}{I_\beta \Omega^2} \int_0^R r_b \, dF_z \, dr_b \tag{2.20}$$

Solving by Fourier series , we can obtain the solution

$$\beta(\Psi) = \beta_0(t) - \beta_{1c}(t) \cos \Psi - \beta_{1s}(t) \sin \Psi \tag{2.21}$$

where β_0 describes the coning angle and the coefficients of the first harmonic β_{1c} and β_{1s} describe the tilting of the rotor tip-path-plane in the longitudinal and lateral directions, respectively.Show in Fig.2.3 and Fig.2.4 .We changing the notation: a instead of β_{1c}, b instead of β_{1s} and a_0 instead of β_0, and letting $\mathbf{a} = (a_0, a, b)$, the motion of tip-path-plane is governed by the following second-order matrix differential equation:

$$\ddot{\mathbf{a}} + \mathbf{D}\dot{\mathbf{a}} + \mathbf{K}\mathbf{a} = \mathbf{F} \tag{2.22}$$

where D is the damping matrix , K is the stiffiness matrix , and F is the forceing term.
To solve Eq.(2.24) , we can write the fuselage equation of motion

$$\dot{u} = -g\theta + X_u u + \cdots + X_a a \tag{2.23}$$
$$\dot{v} = -g\phi + Y_v v + \cdots + Y_b b \tag{2.24}$$
$$\dot{w} = -Z_u u + Z_w w \cdots + Z_{\text{col}}\delta_{\text{col}} \tag{2.25}$$
$$\dot{p} = L_u u + L_v v + \cdots + L_b b \tag{2.26}$$
$$\dot{q} = M_u u + M_v v + \cdots + M_a a \tag{2.27}$$
$$\dot{r} = N_r r + \cdots + N_{\text{ped}}\delta_{\text{ped}} \tag{2.28}$$

where δ_{lat}, δ_{lon}, δ_{ped}, δ_{col} denote the cyclic lateral input, the cyclic longitudinal input, the pedal input and the collective input, respectively. The subscripts in the above equations denote the partial derivative with respect to the subscripted parameters.

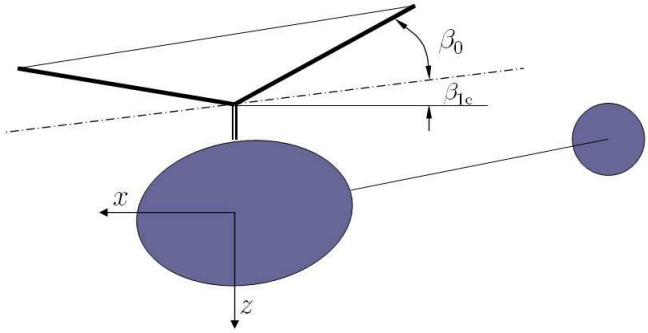

Figure 2.3: Thunder Tip-path-plane rotor representation

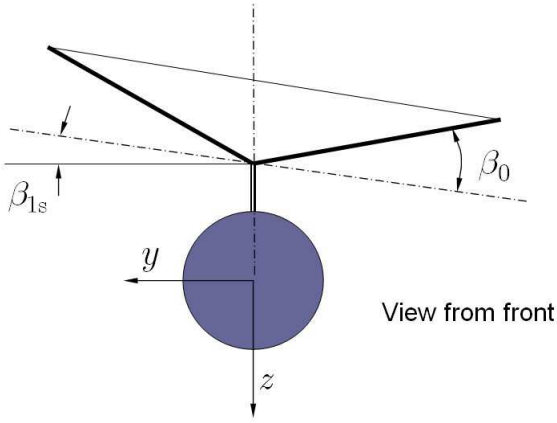

Figure 2.4: Thunder Tip-roll-plane rotor representation

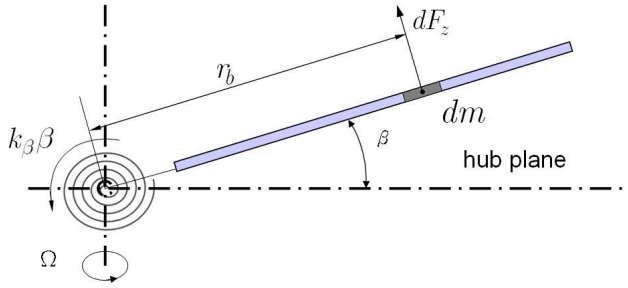

Figure 2.5: Definition of Rotor Parameters

2.4 Yaw Dynamics and Flybar Dynamics

The flybar dynamics is also viewed as a feedback to the main rotor dynamics. Accordingly, the augmented dynamics of the main rotor is then given by

$$\tau_f \dot{a} = -a - \tau_f q + A_b b + A_{\text{lon}}(\delta_{\text{lon}} + K_c c) + A_{\text{lat}}\delta_{\text{lat}} \quad (2.29)$$

$$\tau_f \dot{b} = -b - \tau_f p + B_a a + B_{\text{lat}}(\delta_{\text{lat}} + K_d d) + B_{\text{lon}}\delta_{\text{lon}} \quad (2.30)$$

where τ_f, τ_s are blade time constant of main rotor and tail rotor.

And the dynamics of the flybar is similar to the main rotor and can be written as:

$$\tau_s \dot{c} = -c - \tau_s q + C_{lon}\delta_{lon} \quad (2.31)$$

$$\tau_s \dot{d} = -d - \tau_s p + D_{lat}\delta_{lat} \quad (2.32)$$

Different from a large helicopter, a small-scaled remote rotorcraft is usually equipped with a yaw rate gyro to stabilize the yaw dynamics. We used to view the gyro as a feedback to the yaw dynamics, and the augmented equation of motion can be written as [10]:

$$\dot{r} = N_v v N_r r + N_{\text{ped}}(\delta_{\text{ped}} - r_{fb}) \quad (2.33)$$

$$\dot{r}_{fb} = -K_{r_{fb}} + K_r r \quad (2.34)$$

where r_{fb} denotes the feedback generated by the yaw rate gyro.

2.5 Transfer function in hover

Although Eq.(2.9) has a complete description to the hovering dynamics of a small-scaled helicopter, to practically implement a state-space controller needs powerful calculation capability. As a result, instead of considering

the whole dynamics described in Eq.(2.9) , in hover we intend only to control the four main channels, cyclic lateral input to rolling, cyclic longitudinal input to pitching, pedal input to yawing, and collective pitch input to vertical motions, whose dynamics can be simplified as the following transfer functions [5–7].

$$\frac{p}{\delta_{lat}} = \frac{L_b(B_{lat} + B_d D_{lat})/\tau_s}{s^2 + (1/\tau_s)s + L_b(\tau_f + B_d\tau_s)/\tau_s} \tag{2.35}$$

transfer function for pitch rate response is

$$\frac{q}{\delta_{lon}} = \frac{M_a(A_{lon} + A_c C_{lon})/\tau_s}{s^2 + (1/\tau_s)s + M_a(\tau_f + A_c\tau_s)/\tau_s} \tag{2.36}$$

transfer function for yaw rate response is

$$\frac{r}{\delta_{ped}} = \frac{N_{ped}(s + K_{r_{fb}})}{s^2 + (K_{r_{fb}} - N_r) + (K_r N_{ped} - N_r K_{r_{fb}})} \tag{2.37}$$

and collective transfer function is

$$\frac{\omega}{\delta_{col}} = \frac{Z_{col}}{s - Z_\omega} \tag{2.38}$$

2.6 Overall model

We can integrate those equations into a state-space form, given by

$$\mathbf{M}\dot{\mathbf{x}} \;=\; \mathbf{F}\mathbf{x} + \mathbf{G}\mathbf{u} \tag{2.39}$$

where the states $\mathbf{x} = [u \;\; v \;\; p \;\; q \;\; \phi \;\; \theta \;\; a \;\; b \;\; \omega \;\; r \;\; r_{fb} \;\; c \;\; d]^T$, and the input vector $\mathbf{u} = [\delta_{\text{lat}} \;\; \delta_{\text{lon}} \;\; \delta_{\text{ped}} \;\; \delta_{\text{col}}]^T$. The complete model of the linearized

dynamics for a small-scaled rotorcraft is given by Eq.(2.42)

$$\begin{bmatrix} \dot{u} \\ \dot{v} \\ \dot{p} \\ \dot{q} \\ \dot{\phi} \\ \dot{\theta} \\ \tau_f\dot{a} \\ \tau_f\dot{b} \\ \dot{w} \\ \dot{r} \\ \dot{r_{fb}} \\ \tau_s\dot{c} \\ \tau_s\dot{d} \end{bmatrix} = \begin{bmatrix} X_u & 0 & 0 & 0 & 0 & -g & X_a & 0 & 0 & 0 & 0 & 0 & 0 \\ 0 & Y_v & 0 & 0 & g & 0 & 0 & Y_b & 0 & 0 & 0 & 0 & 0 \\ L_u & L_v & 0 & 0 & 0 & 0 & 0 & L_b & L_w & 0 & 0 & 0 & 0 \\ M_u & M_v & 0 & 0 & 0 & 0 & M_a & 0 & M_w & 0 & 0 & 0 & 0 \\ 0 & 0 & 1 & 0 & 0 & 0 & 0 & 0 & 0 & 0 & 0 & 0 & 0 \\ 0 & 0 & 0 & 1 & 0 & 0 & 0 & 0 & 0 & 0 & 0 & 0 & 0 \\ 0 & 0 & 0 & -\tau_f & 0 & 0 & -1 & A_b & 0 & 0 & 0 & A_c & 0 \\ 0 & 0 & -\tau_f & 0 & 0 & 0 & B_a & -1 & 0 & 0 & 0 & 0 & B_d \\ 0 & 0 & 0 & 0 & 0 & 0 & Z_a & Z_b & Z_w & Z_r & 0 & 0 & 0 \\ 0 & N_v & N_p & 0 & 0 & 0 & 0 & 0 & N_w & N_r & N_{rfb} & 0 & 0 \\ 0 & 0 & 0 & 0 & 0 & 0 & 0 & 0 & 0 & K_r & K_{rfb} & 0 & 0 \\ 0 & 0 & 0 & -\tau_s & 0 & 0 & 0 & 0 & 0 & 0 & 0 & -1 & 0 \\ 0 & 0 & -\tau_s & 0 & 0 & 0 & 0 & 0 & 0 & 0 & 0 & 0 & -1 \end{bmatrix} \begin{bmatrix} u \\ v \\ p \\ q \\ \phi \\ \theta \\ a \\ b \\ w \\ r \\ r_{fb} \\ c \\ d \end{bmatrix}$$

$$+ \begin{bmatrix} 0 & 0 & 0 & 0 \\ 0 & 0 & Y_{ped} & 0 \\ 0 & 0 & 0 & 0 \\ 0 & 0 & 0 & M_{col} \\ 0 & 0 & 0 & 0 \\ 0 & 0 & 0 & 0 \\ A_{lat} & A_{lon} & 0 & 0 \\ B_{lon} & B_{lon} & 0 & 0 \\ 0 & 0 & 0 & Z_{col} \\ 0 & 0 & N_{ped} & N_{col} \\ 0 & 0 & 0 & 0 \\ 0 & C_{lon} & 0 & 0 \\ D_{lat} & 0 & 0 & 0 \end{bmatrix} \begin{bmatrix} \delta_{lat} \\ \delta_{lon} \\ \delta_{ped} \\ \delta_{col} \end{bmatrix} \tag{2.40}$$

Chapter 3

System Identification

The goal of system identification is to achieve the best possible fit of the estimated frequency responses and,ultimately, the vehicle responses ,whth a model that is physically meaningful and that has accuracy well suited for high-bandwidth control design applications.he system identification is one of the useful techniques to reconstruct the plant dynamics. There are a variety of system identification techniques suitable for different kind of problems.

There are a variety of system identification algorithms suitable for different kind of problems. In this project, we select the ARX and PEM model to identify the parameters of our helicopter.

3.1 Data Collection

Data collection is the first and the most important step in system identification.High quality flight data is essentual to successful identification . Taking our investigating problems into consideration, we need flight test data that can stimulate responses at significant frequencies. Therefore,

rules that meet this requirement are very important. In practical experiments, however, it is not easy to obtain data with good quality. Namely we have to consider alternative ways to accomplish this difficult mission.

In addition to the considerations, we need to collect data of

1. Inputs: cyclic lateral δ_{lat}, cyclic longitudinal δ_{lon}, pedal δ_{ped}, and collective δ_{col}
2. Output: Euler angles (roll: ϕ, pitch θ, yaw ψ) , body velocities: (u, v, w) ,angular body rates: (roll p, pitch q, yaw r) , body accelerations: (a_x, a_y, a_z)

We need some equipmen to help collect the flight data , Some equipment must be setup on helicopter and some must setup at ground.These equipment describes as:

- OBC: We choice five different PC-104 standard PC and PC/AT motherboards and expansion cards with our flight computer.
- GPS: The GPS includes antenna and Septentrio PolaRx2@ GPS Receiver. The performance

    1. Position:Vertical: 1.9 m, Horizontal: 1.1 m
    2. Velocity:Vertical: 2.8 mm/s, Horizontal:1.5 mm/s
    3. Update data:Up to 10 Hz raw measurement output rate ,Up to 10 Hz position output rate
    4. Channel:48 hardware channels

- PWM Decoder: The goal is measure the pilot input signal to servo and decode the signal information than we can use to our identiification work.

3.2 What is System Identification

System identification is a general term to describe mathematical tools and algorithms that build dynamical models from measured data. A dynamical mathematical model in this context is a mathematical description of the dynamic behavior of a system or process.

3.3 Introduction to ARX

A common multi-variable ARX model with m inputs and p outputs can written as

$$\begin{aligned} y(t) + A_1 y(t-1) + \cdots + A_n y(t-n_a) = \\ B_1 u(t-1) + \cdots B_n u(t-n_b) + e(t) \end{aligned} \tag{3.1}$$

where the A_i are $p \times p$ matrices and the B_i are $p \times m$ matrices. Eq.(17) can be transformed to a simpler form, given by

$$y(t) = G(q,\theta)u(t) + H(q,\theta)e(t) \tag{3.2}$$

where

$$\begin{aligned} G(q,\theta) &= \mathbf{A}^{-1}(q)\mathbf{B}(q) \\ H(q,\theta) &= \mathbf{A}^{-1}(q) \\ \mathbf{A}(q) &= I + A_1 q^{-1} + \cdots + A_{n_a} q^{-n_a} \\ \mathbf{B}(q) &= B_1 q^{-1} + \cdots + B_{n_b} q^{-n_b} \end{aligned}$$

then define the $(n_a \cdot p + n_b \cdot m)$ by p parameter matrix $\theta = [A_1 \;\; A_2 \;\; \cdots \;\; A_{n_a} \;\; B_1 \;\; \cdots \;\; B_{n_b}]^T$ and the$(n_a \cdot p + n_b \cdot m)$-dimension known data matrix $\varphi(t) = [-y(t-1) \;\; \cdots \;\; -y(t-n_a) \;\; u(t-1) \;\; \cdots \;\; u(t-n_b)]^T$

Then Eq.(15) becomes

$$y(t|\theta) = \varphi^T(t)\theta + e(t) \tag{3.3}$$

Define the cost function

$$\begin{aligned} V_N(\boldsymbol{\theta}, Z^N) &= \frac{1}{N}\sum_{t=1}^{N}\frac{1}{2}\varepsilon^2(t,\boldsymbol{\theta}) \\ &= \frac{1}{N}\sum_{t=1}^{N}\frac{1}{2}[y(t) - \boldsymbol{\varphi}^T(t)\boldsymbol{\theta}]^2 \end{aligned} \tag{3.4}$$

By minimizing the cost function with the least-square method, we are able to solve the parameter θ , and reconstruct the dynamics, given by

$$\begin{aligned} \widehat{\boldsymbol{\theta}}_N^{\mathrm{LS}} &= \arg\min V_N(\boldsymbol{\theta}, Z^N) \\ &= \left[\frac{1}{N}\sum_{t=1}^{N}\boldsymbol{\varphi}(t)\boldsymbol{\varphi}^T(t)\right]^{-1}\frac{1}{N}\sum_{t=1}^{N}\boldsymbol{\varphi}(t)y(t) \end{aligned} \tag{3.5}$$

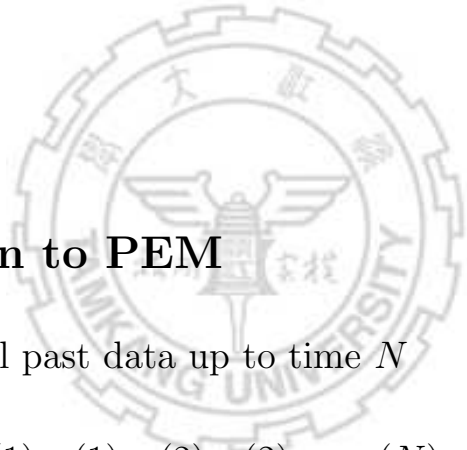

3.4 Introduction to PEM

Define the collection all past data up to time N

$$Z^N = \{u(1), y(1), u(2), y(2), \cdots u(N), y(N)\} \tag{3.6}$$

The basic idea of prediction error is to describe the model as a predictor of the next output$\hat{y}_N(t \mid \theta) = f(Z^{t-1}, \theta)$,where$f(Z^t, \theta)$ is the arbitrary function of the past observed data and parameters to estimate. By minimizing the distance between the predicted outputs (according to parameter θ) and the measured outputs (or the cost function), given by

$$\hat{\theta}_N = argmin V_N(\theta) \tag{3.7}$$

$$V_N(\theta) = \sum_{t=1}^{N}\ell(y(t) - f(Z^{t-1}, \theta)) \tag{3.8}$$

we are able to estimate the parameters using maximum likelylood method. The actual calculation of the minimizing argument can be complicated.

We use the Gauss-Newton method:

$$\hat{\theta}^{i+1} = \hat{\theta}^{i} - \mu_i \frac{V_N^{'}(\hat{\theta}^{i})}{V_N^{''}(\hat{\theta}^{i})} \tag{3.9}$$

where

$$\begin{aligned} V_N^{'}(\theta) &= \frac{dV_N^{'}(\theta)}{d\theta} \\ &= -\frac{1}{N}\sum y(t) - \hat{y}(t \mid \theta))\psi(t,\theta) \\ & V_N^{''}(\theta) \approx \frac{1}{N}\psi(t,\hat{\theta}^{i})\psi^{T}(t,\hat{\theta}^{i}) \\ \psi(t,\theta) &= \frac{\partial}{\partial\theta}\hat{y}(t \mid \theta) \end{aligned} \tag{3.10}$$

Here μ_i is a scalar, adjusted so that the criterion $V_N(\theta^{(i+1)}) < V_N(\theta^{(i)})$The two algorithms have been realized and developed as a toolbox in Matlab. In this research we simply apply our flight test data to the toolbox and analyze the results

3.5 Comparison between ARX and PEM

Even though we can obtain linear dynamics models of R-90 from both ARX and PEM, there are still fundamental differences between these two algorithms. First of all, ARX identify parameters via a cost function while PEM via maximum likely hood method. Second, ARX identify parameters via a linear model with PEM a general model, which makes PEM extend its applications to a nonlinear region. Third, to stimulate the spectra of a

helicopter so that a better result using ARX is attainable, we have to do a very sophisticated maneuver in flight test, leading to higher possibility of accidents when doing flight test. As a result, PEM is an alternative choice since it identifies parameters using data history and given model, which doesn't require sophisticated maneuver and can lower down the possibility of accidents.

Chapter 4

Identified Results of linearized system

Flight data of this experiment.We only do roll and pitch in movement of the helicopter.Because that the helicopter is difficult to control . And that in our helicopter used for experiment in yaw channel have a gyroscope , it can help us to stability of the posture . So the result that we distinguish out may be distorted .

In this section figures and parameters, listed in tables, of identified parameters are given. At beginning we provide the Bode plots of the two channels identified using ARX and CIFER. Lists of identified parameters and discussions are then provided.

4.1 Flight Test Rules

When we use ARX and CIFER to identification our data in hover, it has some rules . The test rules are detailed in Ref. [1], and we just briefly introduce here. The principle considerations are:

1. Sufficient excitation throughout frequency range of interest
2. Record length and sampling rate
3. Maintain the operation within range of linear dynamics
4. Minimize correlation among inputs
5. Minimize amount of feedback. During our experiment

all control inputs and all vehicle state variables where recorded and sampled at 10 Hz .At least two continuous waves as show in Fig.4.1 and Fig.4.2 . In addition , it low-frequency is near 0.1-2 rad/sec and high-frequency is near 8-14 rad/sec . In our experiment, the input signals are obtained form the measurement of the PWM signal, whichis the signal that drives the servos. Thus, we use the percentage input, calculated from the PWM signals, between $\pm 100\%$ to replace the real pitch-angle input.

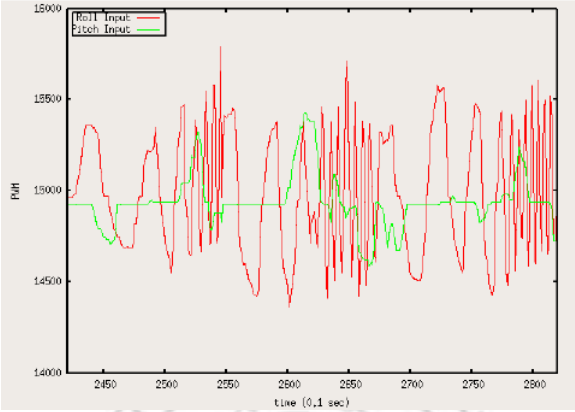

Figure 4.1: The Roll Sine Input

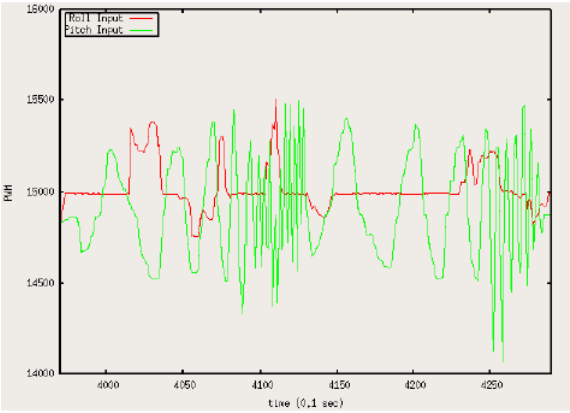

Figure 4.2: The Pitch Sine Input

4.2 Identified with ARX

Our flight data input use OBC send automatically separately the sine input.signal on roll and pitch. Show in Fig.4.1 and Fig.4.2 . The Fig.4.1 use roll sine input , during flying , the persons who control try one's best to avoid other movements . So in some period , we Can see green line (pitch) segment levels the state . Namely the introduction without pitch signal is interfered this period . But some times still unable to totally avoid .

Then we use the data as show in Fig.4.1 with ARX . We can find out that it is a two order system from Fig.4.3 , and can get the natural frequencies $\omega_n \approx 20.6$ and damping ratios $\xi \approx 0.16 - 0.19$ too.

Next we use the data as show in Fig 4.2 with ARX .The data use OBC send automatically separately the sine signal on pitch . We can see that during flying the red line (roll) segment levels the state . Namely the introduction without roll signal is interfered this period . But some times still unable to totally avoid too . We also can find out that it is a two order system from Fig.4.4 and can get natural frequencies $\omega_n \approx 11$ and damping ratios $\xi \approx 0.39 - 0.4$. In order to prove the result accuracy that uses with ARX identification technology . We use the CIFER to confirm the accuracy of the result in next section.

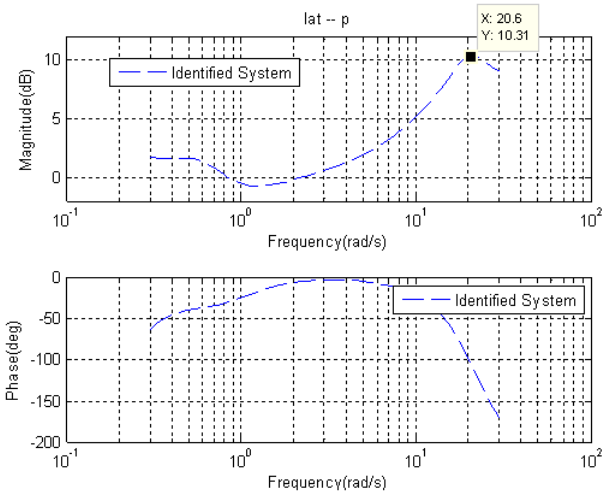

Figure 4.3: The Bode plot of $p/\delta_{lat} from ARX$

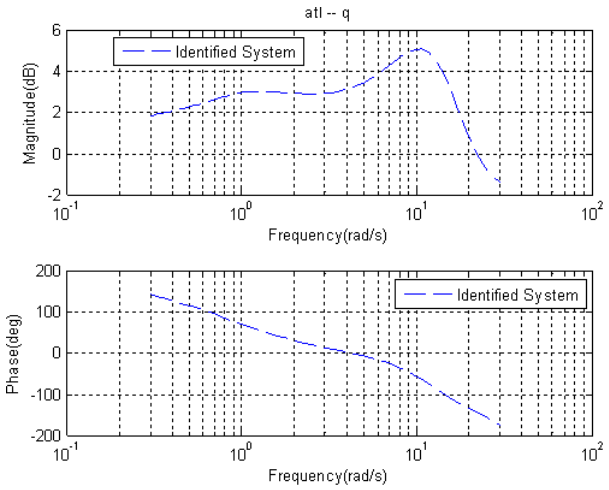

Figure 4.4: The Bode plot of q/δ_{lon} from ARX

4.3 Identified with CIFER

when we identified with CIFER , we use the same flight data as show Fig.4.1 and Fig.4.2 . Then it can find out that it is a two order system in roll channel , can get natural frequencies $\omega_n = 19.649$ and damping ratios $\xi = 0.1679$ from Fig.4.5 and Fig.4.6 . And can find out that is atwo order system in pitch channel too . See the Fig.4.7 and Fig.4.8 can get the natural frequencies $\omega_n = 19.649$ and damping ratios $\xi = 0.1679$. The Fig.4.9 and Fig.4.10 are coherence plot about input and output . The coherence γ_{uy} indicates how much an output y is linearly correlated with a particular input u as a function of frequency . The coherence is computed from the cross-spectrum G_{uy} and the input and output auto-spectra G_{uu} and G_{yy} , respectively

$$\gamma_{uy}^2 = \frac{|G_{uy}|^2}{G_{uu}G_{yy}} \leq 1 \tag{4.1}$$

If greater than 0.6 , we can get better identification result . In our sine input data can see that the period longest about five seconds . So frequency is about 1.256 rad/s , We can find roll part good after this frequency from the coherence plot (above 0.6) , but it is bad in pitch part .

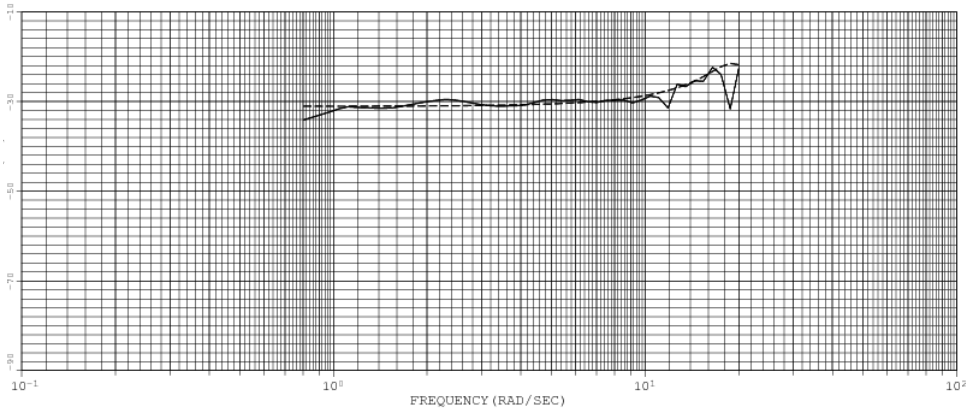

T1124_COM_ABCDE_lat_p
Fit
Cost: 26.231 Gain(HF): 0.107913E+02 S.S.: 0.279505E-01 Delay: 0.0292

	NUMERATOR		DENOMINATOR	
	REAL	IMAG	REAL	IMAG
1			-0.32985E+01	0.19370E+02
2		(Z=0.1679 , W= 19.6490 (Rad/sec))		

Figure 4.5: The Bode magnitude plot of p/δ_{lat} from CIFER

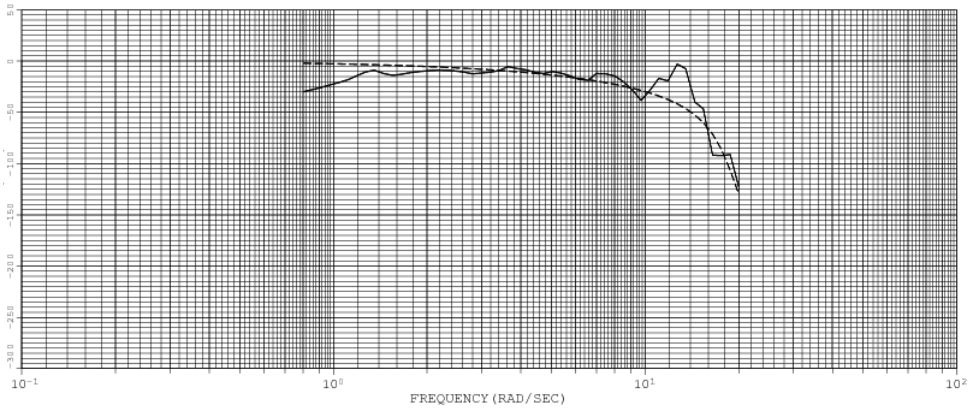

T1124_COM_ABCDE_lat_p
Fit
Cost: 26.231 Gain(HF): 0.107913E+02 S.S.: 0.279505E-01 Delay: 0.0292

	NUMERATOR		DENOMINATOR	
	REAL	IMAG	REAL	IMAG
1			-0.32985E+01	0.19370E+02
2		(Z=0.1679 , W= 19.6490 (Rad/sec))		

Figure 4.6: The Bode phase plot of p/δ_{lat} from CIFER

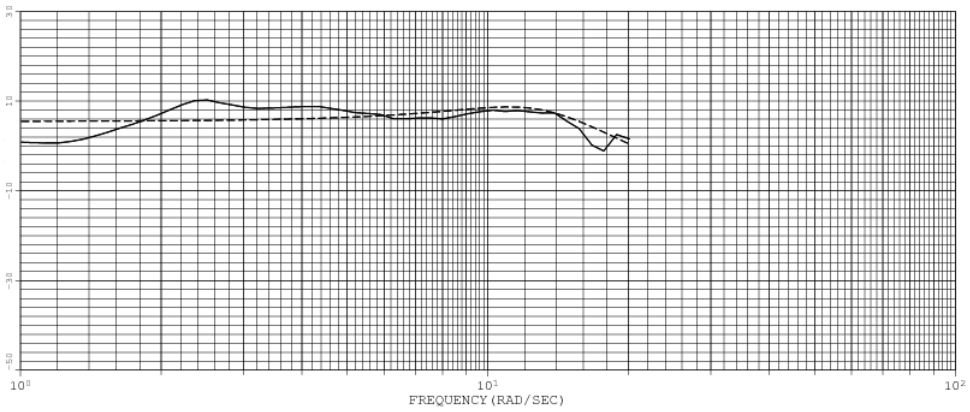

T1124q_COM_ABCDE_lon_q
Fit
Cost: 44.978 Gain(HF): 0.318609E+03 S.S.: 0.187700E+01 Delay: -.0202

	NUMERATOR		DENOMINATOR	
	REAL	IMAG	REAL	IMAG
1			-0.48378E+01	0.12097E+02
2		(Z=0.3713 , W= 13.0286 (Rad/sec))		

Figure 4.7: The Bode magnitude plot of q/δ_{lon} from CIFER

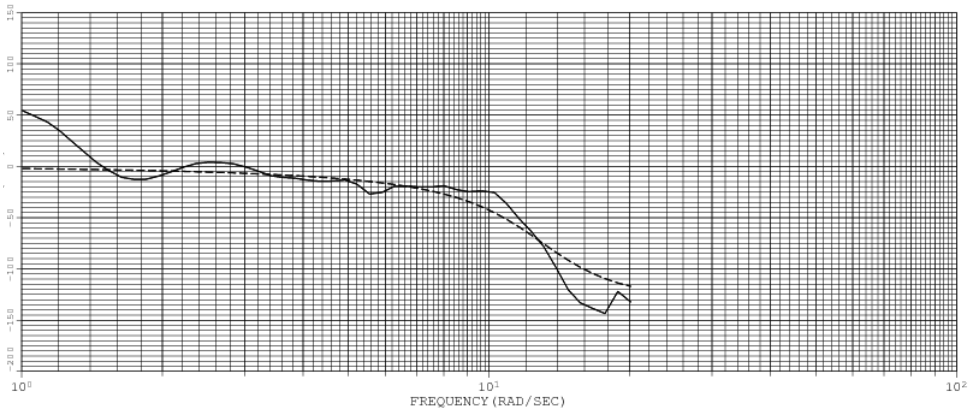

T1124q_COM_ABCDE_lon_q
Fit
Cost: 44.978 Gain(HF): 0.318609E+03 S.S.: 0.187700E+01 Delay: -.0202

	NUMERATOR		DENOMINATOR	
	REAL	IMAG	REAL	IMAG
1			-0.48378E+01	0.12097E+02
2		(Z=0.3713 , W= 13.0286 (Rad/sec))		

Figure 4.8: The Bode phase plot of q/δ_{lon} from CIFER

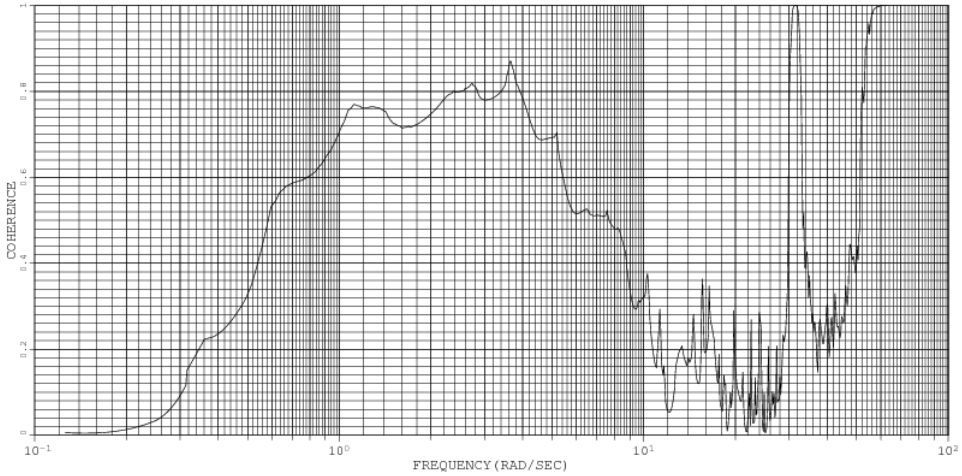

Figure 4.9: The Coherence plot of p/δ_{lat}

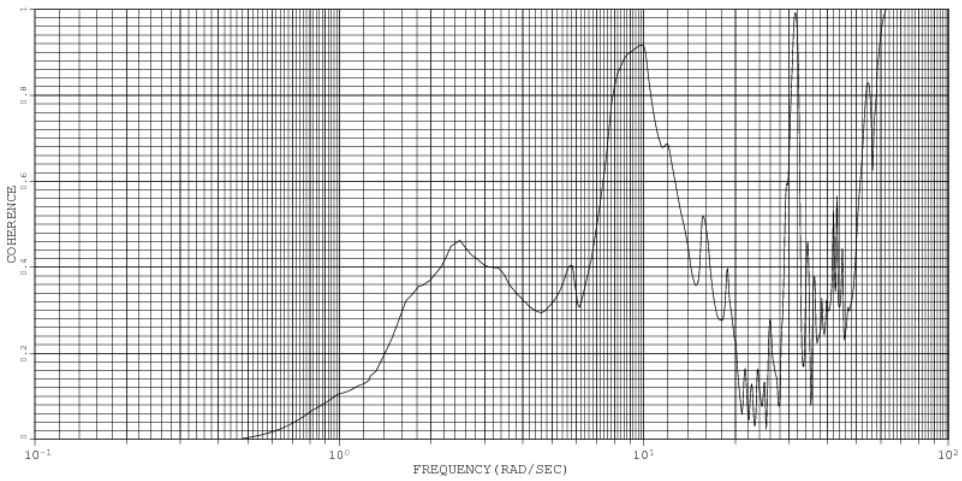

Figure 4.10: The Coherence plot of q/δ_{lon}

4.4 Identified Parameters with ARX , CIFER ,PEM

In previous sections we used ARX and CIFER to identify the model . Now, we will use PEM to identify the R90 model. The new version of *System Identification Toolbox* in Matlab 2007a make many improvement and include function of nonlinear system identification. This version of toolbox was much more intact. The command of PEM will help process our problem.

Identified parameters are given in the following tables. Table.4.2 and Table.4.3 provide the damping ratios and natural frequencies for the lateral and longitudinal channels, respectively . We can get the R-50 parameters from [1], and use scaling rule to get consulting value . The scaling rule is according to on physical characteristic , about the rotor length L_p,etc .We use Froude scaling and March scaling , The table.4.1 show the scaling rules . We will get vale with R-50 model and guess value of R-90 , when $N = 2$ show in table.4.2 and 4.3 .

Dimension	Froude	March
Length	$L_m = \frac{L_p}{N}$	$L_m = \frac{L_p}{N}$
Time	$T_m = \frac{T_p}{\sqrt{N}}$	$T_m = \frac{T_p}{N}$
Velocity	$V_m = \frac{V_p}{\sqrt{N}}$	$V_m = V_p$
Weight	$W_m = \frac{W_p}{N^3}$	$W_m = \frac{W_p}{N^3}$
Moment of inertia	$I_m = \frac{I_p}{N^5}$	$I_m = \frac{I_p}{N^5}$
Frequency	$\omega_m = \omega_p\sqrt{N}$	$\omega_m = \omega_p\sqrt{N}$

Table 4.1: Scaling rules of Froude and March

The complete parameters, identified using different algorithms, are listed in Table.4 for comparison.Where a and longitudinal are related , b and lateral are related in hover . So we define $B_a = A_b = B_{lon} = A_{lat} = 0$, other parameters can according to the transfer function from chapter.2 . If

the parameters are in transfer function for pitch rate response , can believe it is relatively correct in result of PEM about pitch . If the parameters are in transfer function for roll rate response , can believe it is relatively correct in result of PEM about roll As this rule we can get these parameters $L_b, B_{lat}, B_d, D_{lat}$ is subject to roll , and these parameters $M_a, A_{lon}, A_c, C_{lon}$, is subject to pitch , Because our flight data just have roll and pitch channel . So the other parameter have not consulted the rule of depending on temporarily .That the values of most parameters are consistent through out different identification algorithms. However, some of them are still inconsistent. As a result, more flight tests should be performed in order to verify the correctness of those parameters.

	ξ	ω_n
ARX	0.16-0.19	20.6
CIFER	0.1679	19.6490
R-50	0.11	10
Consulting value	0.15-0.22	14-20

Table 4.2: Parameters for lateral channel

	ξ	ω_n
ARX	0.39-0.4	11
CIFER	0.3713	13.0286
R-50	0.14	9
Consulting value	0.19-0.28	12.73-18

Table 4.3: Parameters for longitudinal channel

Parameter	PEM(roll)	PEM(pitch)	ARX	Parameter	PEM(roll)	PEM(pitch)	ARX
τ_f	0.0268	0.047	0.052	τ_s	0.2492	0.1122	0.22
X_u	-0.6417	-0.209	-0.05	Y_v	-0.1021	-0.111	-0.154
L_u	-0.2391	0.0047	-0.14	L_v	0.2133	0.1048	-0.14
L_b	326	325.99	320	M_u	0.1134	0.1347	-0.056
M_v	0.1884	-0.069	-0.058	M_a	203.99	203.99	204
B_a	0	0	0	B_d	1.1317	0.1336	1.51
A_b	0	0	0	A_c	1.0357	0.9303	1.51
Z_a	-9.7501	-9.7499	-9.57	Z_b	-131	-131	-131
Z_w	-2.0572	-0.9201	-0.614	Z_r	0.7449	0.9048	0.93
N_v	-0.0079	0.0963	0.03	N_w	0.9255	1.006	0.086
N_p	-3.4789	-3.506	-3.53	N_r	-4.7137	-0.7053	-0.4
K_r	-0.7128	0.723	2.16	A_{lat}	0	0	0
A_{lon}	0.1734	0.1102	0.53	B_{lat}	0.0473	-0.0021	0.42
B_{lon}	0	0	0	C_{lon}	0.0348	0.1336	0.11
D_{lat}	-0.0995	-0.0051	0.11	Z_{col}	-45.722	-45.77	-45.8
N_{col}	-2.8524	-2.9365	-3.33	N_{ped}	33.1027	33.1052	9.16

Table 4.4: List of complete parameters

Chapter 5

Nonlinear Dynamics

In the preceding sections, the linear model of R-90 as well as its parameters are identified and provided. However, the application of a linear model is usually limited to the neighborhood of the nominal states. For a complex machine like a helicopter, this implies that a linear model only helps to maneuver under certain *simple and fixed* circumstance. For example, control to remain at the hovering state. If one wants to maneuver the helicopter from state to state, say, from hover to cruise, a linear model cannot afford enough information.

An alternative solution to the problem of states transferring is to develop a nonlinear model, which usually has wider range of applications. However, due to the complexity of the coupling effects between aerodynamics and helicopter dynamics, a pure nonlinear model is hardly to obtain. Instead, we are going to use a linear model but with *nonlinear parameters*. Although this may limit the application of this model, we still can consider the problem of states transferring through updating the parameters frequently.

We don't intend to derive the linear model with nonlinear parameters (will be briefed as "*the nonlinear model*" in the following texts), which

is already derived in Ref. [14] and listed in teh following section. In this project we are going to apply the system identification methodology to obtain the values of the constants in the nonlinear parameters.

5.1 Nonlinear Parameters list

In Eq. (2.42) we have introduced several linearized parameters, such as ($X_u = \frac{\partial X}{\partial u}$, $X_v = \frac{\partial X}{\partial v}$, ...,$N_{col} = \frac{\partial N}{\partial \delta_{col}}$). Those parameters are treated as fixed values in every flight state in the preceding sections. In this section, however, we are going to further expand those parameters into nonlinear terms, and investigate the most primary constants in those parameters. The expansion of those parameters are provided in Ref. [14] and listed in the following:

$$\begin{aligned}
X_u &= -\rho A_b (\Omega R)^2 \frac{\partial C_H/\sigma}{\partial a}\frac{\partial a}{\partial \mu}\frac{\partial \mu}{\partial u} \\
&= -\rho A_b (\Omega R)^2 \frac{3}{2}\frac{C_T}{\sigma}(1 - \frac{a_1}{18}\frac{\theta_{.75}}{\frac{C_T}{\sigma}})(\frac{8}{3}\theta_0 + 2\theta_1 - 2\frac{\nu_1}{\Omega R})(\frac{1}{\Omega R})_M \quad (5.1) \\
X_a &= -\rho A_b (\Omega R)^2 \frac{\partial C_H/\sigma}{\partial a} \\
&= -\rho A_b (\Omega R)^2 \frac{3}{2}\frac{C_T}{\sigma}(1 - \frac{a_1}{18}\frac{\theta_{.75}}{\frac{C_T}{\sigma}}) \quad (5.2) \\
Y_v &= -\rho A_b (\Omega R)^2 \frac{\partial C_H/\sigma}{\partial a}\frac{\partial a}{\partial \mu}\frac{\partial \mu}{\partial u} + \rho A_b (\Omega R)^2 \frac{\partial C_T/\sigma}{\partial \lambda'}\frac{\partial \lambda'}{\partial v_1} \\
&= -\rho A_b (\Omega R)^2 \frac{3}{2}\frac{C_T}{\sigma}(1 - \frac{a_1}{18}\frac{\theta_{.75}}{\frac{C_T}{\sigma}})(\frac{8}{3}\theta_0 + 2\theta_1 - 2\frac{\nu_1}{\Omega R}) \\
&\quad + \rho A_b (\Omega R)^2 \frac{1}{\frac{8}{a_1} + \frac{\sqrt{\frac{\sigma}{2}}}{\sqrt{\frac{C_T}{\sigma}}}}(\frac{-1}{\Omega R})_T \quad (5.3)
\end{aligned}$$

$$
\begin{aligned}
Y_b &= \rho A_b(\Omega R)^2 \frac{\partial C_y/\sigma}{\partial b} \\
&= \rho A_b(\Omega R)^2 \frac{3}{2}\frac{C_T}{\sigma}(1-\frac{a_1}{18}\frac{\theta_{.75}}{\frac{C_T}{\sigma}}) \qquad (5.4) \\
Y_{ped} &= \rho A_b(\Omega R)^2 \frac{\partial C_T/\sigma}{\partial \theta_0} \\
&= \rho A_b(\Omega R)^2 \frac{3}{8}a_1 \qquad (5.5) \\
Z_\omega &= -\rho A_b(\Omega R)^2 \frac{\partial C_T/\sigma}{\partial \lambda'}\frac{\partial \lambda'}{\partial \omega} \\
&= -\rho A_b(\Omega R)^2 \frac{1}{\frac{8}{a_1}+\frac{\sqrt{\frac{\sigma}{2}}}{\sqrt{\frac{C_T}{\sigma}}}}(\frac{1}{\Omega R})_T \qquad (5.6) \\
Z_{col} &= -\rho A_b(\Omega R)^2 \frac{\partial C_T/\sigma}{\partial \theta_0} \\
&= -\rho A_b(\Omega R)^2 \frac{a_1}{6} \qquad (5.7) \\
L_u &= (\frac{dL}{db})_M \frac{\partial b}{\partial \mu}\frac{\partial \mu}{\partial u} + \rho A_b(\Omega R)^2 \frac{\partial C_y/\sigma}{\partial b}\frac{\partial b}{\partial \mu}\frac{\partial \mu}{\partial u}b_M \\
&= (\frac{dL}{db})_M \frac{4}{3}a_1(\frac{1}{\Omega R})_M \\
&\quad +\rho A_b(\Omega R)^2 \frac{3}{2}\frac{C_T}{\sigma}(1-\frac{a_1}{18}\frac{\theta_{.75}}{\frac{C_T}{\sigma}})\frac{4}{3}a_1(\frac{1}{\Omega R})_M b_M \qquad (5.8) \\
L_v &= -(\frac{dM}{da})_M \frac{\partial a}{\partial \mu}\frac{\partial \mu}{\partial u} - \rho A_b(\Omega R)^2 \frac{\partial C_H/\sigma}{\partial a}\frac{\partial a}{\partial \mu}\frac{\partial \mu}{\partial u}b_M \\
&\quad -\rho A_b(\Omega R)^2 \frac{\partial C_H/\sigma}{\partial a}\frac{\partial a}{\partial \mu}\frac{\partial \mu}{\partial u} \\
&\quad +\rho A_b(\Omega R)^2 \frac{\partial C_T/\sigma}{\partial \lambda'}\frac{\partial \lambda'}{\partial v}b_T \\
&= -(\frac{dM}{da})_M(\frac{8}{3}\theta_0+2\theta_1-2\frac{\nu_1}{\Omega R})(\frac{1}{\Omega R})_M \\
&\quad -\rho A_b(\Omega R)^2 \frac{3}{2}\frac{C_T}{\sigma}(1-\frac{a_1}{18}\frac{\theta_{.75}}{\frac{C_T}{\sigma}}) \\
&\quad (\frac{8}{3}\theta_0+2\theta_1-2\frac{\nu_1}{\Omega R})(\frac{1}{\Omega R})_M b_M - \rho A_b(\Omega R)^2 \frac{3}{2}\frac{C_T}{\sigma}(1-\frac{a_1}{18}\frac{\theta_{.75}}{\frac{C_T}{\sigma}}) \\
&\quad (\frac{8}{3}\theta_0+2\theta_1-2\frac{\nu_1}{\Omega R})(\frac{1}{\Omega R})_M^{38} \\
&\quad +\rho A_b(\Omega R)^2 \frac{1}{\frac{8}{a_0}+\frac{\sqrt{\frac{\sigma}{2}}}{\sqrt{\frac{C_T}{\sigma}}}}(\frac{-1}{\Omega R})_T b_T \qquad (5.9)
\end{aligned}
$$

$$L_b = (\frac{dL}{db})_M \tag{5.10}$$

$$\begin{aligned} L_\omega &= -\rho A_b(\Omega R)^2 \frac{\partial C_T/\sigma}{\partial \lambda'} \frac{\partial \lambda'}{\partial \omega} Y_M \\ &= -\rho A_b(\Omega R)^2 \frac{1}{\frac{8}{a_1} + \frac{\sqrt{\frac{\sigma}{2}}}{\sqrt{\frac{C_T}{\sigma}}}} (\frac{1}{\Omega R})_T \end{aligned} \tag{5.11}$$

$$\begin{aligned} M_u &= (\frac{dM}{da})_M \frac{\partial a}{\partial \mu}\frac{\partial \mu}{\partial u} + \rho A_b(\Omega R)^2 \frac{3}{2}\frac{C_T}{\sigma}(1 - \frac{a_1}{18}\frac{\theta_{.75}}{\frac{C_T}{\sigma}})(\frac{8}{3}\theta_0 + 2\theta_1 - 2\frac{\nu_1}{\Omega R})(\frac{1}{\Omega R})_M \\ &= (\frac{dM}{da})_M \frac{3}{2}\frac{C_T}{\sigma}(1 - \frac{a_1}{18}\frac{\theta_{.75}}{\frac{C_T}{\sigma}}) \\ &\quad (\frac{8}{3}\theta_0 + 2\theta_1 - 2\frac{\nu_1}{\Omega R})(\frac{1}{\Omega R})_M \\ &\quad + \rho A_b(\Omega R)^2 \frac{3}{2}\frac{C_T}{\sigma}(1 - \frac{a_1}{18}\frac{\theta_{.75}}{\frac{C_T}{\sigma}})(\frac{8}{3}\theta_0 + 2\theta_1 - 2\frac{\nu_1}{\Omega R})(\frac{1}{\Omega R})_M b_M \end{aligned} \tag{5.12}$$

$$\begin{aligned} M_v &= (\frac{dL}{db})_M \frac{\partial b}{\partial \mu}\frac{\partial \mu}{\partial u} + \rho A_b(\Omega R)^2 \frac{\partial C_y/\sigma}{\partial b}\frac{\partial b}{\partial \mu}\frac{\partial \mu}{\partial u} b_M \\ &\quad + \rho A_b(\Omega R)^2 \frac{\partial C_Q/\sigma}{\partial \lambda'}\frac{\partial \lambda'}{\partial v} \\ &= (\frac{dL}{db})_M \frac{4}{3}a_1(\frac{1}{\Omega R})_M + \rho A_b(\Omega R)^2 \frac{3}{2}\frac{C_T}{\sigma}(1 - \frac{a_1}{18}\frac{\theta_{.75}}{\frac{C_T}{\sigma}})\frac{4}{3}a_1(\frac{1}{\Omega R})_M b_M \\ &\quad + \frac{a_1}{4}(\theta.75 - 2\frac{\nu_1}{\Omega R})(\frac{1}{\Omega R})_T \end{aligned} \tag{5.13}$$

$$M_a = (\frac{dM}{da})_M \tag{5.14}$$

$$\begin{aligned} M_\omega &= -\rho A_b(\Omega R)^2 \frac{\partial C_T/\sigma}{\partial \lambda'}\frac{\partial \lambda'}{\partial \omega} l_M \\ &= -\rho A_b(\Omega R)^2 \frac{1}{\frac{8}{a_1} + \frac{\sqrt{\frac{\sigma}{2}}}{\sqrt{\frac{C_T}{\sigma}}}} (\frac{1}{\Omega R})_T l_M \end{aligned} \tag{5.15}$$

$$\begin{aligned} M_{col} &= \rho A_b(\Omega R)^2(a + i_M)\frac{\partial C_T}{\partial \theta_0} b_M - \rho A_b(\Omega R)^2 \frac{\partial C_T}{\partial \theta_0} l_M \\ &= \rho A_b(\Omega R)^2(a + i_M)\frac{a_1}{6} b_M - \rho A_b(\Omega R)^2 \frac{a_1}{6} l_M \end{aligned} \tag{5.16}$$

$$
\begin{aligned}
N_v &= -\rho A_b(\Omega R)^2 \frac{\partial C_T/\sigma}{\partial \lambda'}\frac{\partial \lambda'}{\partial v} l_T \\
&= -\rho A_b(\Omega R)^2 \frac{1}{\frac{8}{a_1}+\frac{\sqrt{\frac{\sigma}{2}}}{\sqrt{\frac{C_T}{\sigma}}}} (\frac{-1}{\Omega R})_T l_T \qquad (5.17)\\
N_p &= -\rho A_b(\Omega R)^2 \frac{\partial C_T/\sigma}{\partial \lambda'}\frac{\partial \lambda'}{\partial v} b_T l_T \\
&= -\rho A_b(\Omega R)^2 \frac{1}{\frac{8}{a_1}+\frac{\sqrt{\frac{\sigma}{2}}}{\sqrt{\frac{C_T}{\sigma}}}} (\frac{-1}{\Omega R})_T b_T l_T \qquad (5.18)\\
N_\omega &= -\rho A_b(\Omega R)^2 \frac{\partial C_Q/\sigma}{\partial \lambda'}\frac{\partial \lambda'}{\partial v} \\
&= \rho A_b(\Omega R)^2 \frac{1}{\frac{8}{a_1}+\frac{\sqrt{\frac{\sigma}{2}}}{\sqrt{\frac{C_T}{\sigma}}}} (\frac{1}{\Omega R})_T \\
N_r &= \rho A_b(\Omega R)^2 \frac{\partial C_T/\sigma}{\partial \lambda'}\frac{\partial \lambda'}{\partial v} l_T l_T + 2\rho A_b(\Omega R) R^2 \frac{C_Q}{\sigma} \\
&= \rho A_b(\Omega R)^2 \frac{1}{\frac{8}{a_1}+\frac{\sqrt{\frac{\sigma}{2}}}{\sqrt{\frac{C_T}{\sigma}}}} (\frac{-1}{\Omega R})_T l_T l_T + 2\rho A_b(\Omega R) R^2 \frac{C_Q}{\sigma} \qquad (5.19)\\
N_{ped} &= -\rho A_b(\Omega R)^2 \frac{\partial C_T/\sigma}{\partial \theta_0} l_T \\
&= -\rho A_b(\Omega R)^2 \frac{a_1}{6} \qquad (5.20)\\
N_{col} &= \rho A_b(\Omega R)^2 \frac{\partial C_Q/\sigma}{\partial \theta_0} \\
&= \rho A_b(\Omega R)^2 \frac{a_1}{4}\sqrt{\frac{\sigma a_1 \theta_t}{8}} \qquad (5.21)
\end{aligned}
$$

In addition to the listed parameters, we still have Z_a, Z_b, Z_r that don't

have expansions. Therefore, those will still be treated as independent parameters.

5.2 Known and Unknown Parameters

Although there are many parameters to be identified, they can categorize into two groups: the *known* and *unknown* group. Here, the *known* parameters are defined as those that we can measure through a simple experiment, such as length or area, and those that we can obtain from mathematical derivation or existing database, such as density of atmosphere, which are listed in Table 5.2. The other parameters are categorized into the *unknown* parameters since they must be obtained via flight test and system identification methodology, which are listed in Table 5.2.

The unknown parameters are going to be identified using PEM methodology. However, due to the hardware problems the flight test is already scheduled but not performed. As a result, the identification of those parameters will be scheduled as future work.

	R-90
Rotor speed	1850 rpm
Full length of fuselage	1410 mm
Full width of fuselage	190 mm
Main rotor Diameter	1550 mm
Tail rotor Diameter	260 mm
Flybar Diameter	660 mm
Total Height	465 mm
Full equipped weight	4.8 kg
Maximum Payload	15 kg

Table 5.1: Characteristics of R-90

solidity of rotor	σ
slope of lift curve	a_1
three-quater pitch angle	$\theta_{.75}$
average pitch at the center of rotation	θ_0
pitch at the blode tip	θ_t
coefficient of thrust	C_T
coefficient of torque	C_Q
slope of L to b	$(\frac{dL}{db})_M$
slope of M to a	$(\frac{dM}{da})_M$
incidence	i_m
The dished between main rotor and z-axis	l_M
The dished between main rotor and x-axis	b_M
The dished between tail rotor and z-axis	l_T
The dished between tail rotor and x-axis	b_T

Table 5.2: Unknown Parameters

Chapter 6

Conclusion and Future Work

6.1 Conclusion

In this project, we first review the equations of motion for small-scales rotorcraft R-90, which later help the work of the identification. Then we use various system identification techniques, including ARX, CIFER, and PEM, to reveal dynamical parameters, and verify the results by comparing those from different identification algorithms. Most of the identified parameters are shown to be consistent, even though some of them still need more flight tests to confirm. The introduction of PEM in this project can be extended to the nonlinear scheme later on. We also investigate the nonlinear model in the last chapter. All the nonlinear parameters can be categorized into two groups: the *known* and *unknown* group, between which the unknown group can be obtained via identification methodology. One potential application of our work is the controller design for autonomous hover.

6.2 Future Work

In this project, we already find linear parameters of R-90 in the hover flight. We will refine the nonlinear grey model to get good results and use PEM to identify nonlinear parameters of R-90 in the future.

Bibliography

[1] B. Mettler, Identification modeling and characteristics of miniature rotorcraft. Kluwer Academic Publishers, Boston,2003.

[2] R. Chen, Effects of Primary Rotor Parameters on Flapping Dynamics, Technical Report TP-1431, NASA, 1980.

[3] B. Mettler, C. Dever and E. Feron, Identification Modeling, Flying Qualities, and Dynamic Scaling of Miniature Rotorcraft, NATO Systems Concepts and Integration Symposium, Berlin, 2002.

[4] G. D. Padfield, Helicopter flight dynamics : the theory and application of flying qualities and simulation modelling, Blackwell Science, 1996.

[5] Hamel, P. G. and Kaletka, J., Advances in Rotorcraft System Identification, Progress in Aerospace Sciences, Vol. 33, No. 3/4, 1997, pages 259-285, 1997.

[6] H. Baruh, Analytical Dynamics, McGraw-Hill, 1999.

[7] S. K. Kim and D. M. Tilbury, Mathematical Modeling and Experimental Identification of an Unmanned Helicopter Robot with Flybar Dynamics, Journal of Robotic Systems, Vol. 21(3):p 95-116, 2004.

[8] B. Mettler, M. B. Tischler, and T. Kanade, System Identification Modeling of a Small-Scale Unmanned Rotorcraft for Flight Control Design, Journal of the American Helicopter Society, Vol. 47(1):50.

[9] B. Mettler, M. B. Tischler, and T. Kanade, System Identification of a Model-Scale Helicopter, Technical Report CMU-RI-TR-00-03, Robotics Institute, Carnegie Mellon University, January 2000.

[10] J. C. Morris, M. van Nieuwstadt, and P. Bendotti. Identification And Control Of A Model Helicopter In Hover. American Control Conference, 1994, Vol. 2:p 1238-1242.

[11] R. W. Prouty. Helicopter Performance, Stability, and Control, Robert E. Krieger Company, INC., 1990.

[12] M. B. Tischler, System identification requirements for high-bandwidth rotorcraft flight control system design, Journal of Guidance, Control, and Dynamics, Vol. 13(5):p 835-841, 1990.

[13] J. H. Tseng. System identification of unmanned helicopter: Applications to R-90. Master's thesis, Tamkang University, 2007

[14] R. W. Prouty, Helicopter Performance , Stability , and Control ,Robert E.Krtegrt Publlshing Company Malabar ,Horida

[15] Lennart Ljung, "Prediction Error Estimation Methods". Received January 5,2001.